Research Performance Progress Report

SUBMITTED TO

U. S. Department of Energy
National Energy Technology Laboratory

WORK PERFORMED UNDER AGREEMENT

DE-FE0013919

Project title: **Mechanisms for Methane Transport and Hydrate Accumulation in Coarse-Grained Reservoirs**

SUBMITTED BY
Prof. Hugh Daigle, PI
Phone: 512-471-3775
Fax: 512-471-9605
daigle@austin.utexas.edu

January 27, 2017

DUNS number: 1702302390000

RECIPIENT ORGANIZATION
University of Texas at Austin
200 E Dean Keeton St., Stop C0300
Austin, TX 78712-1585

PROJECT PERIOD: October 1, 2013 – September 30, 2017

REPORTING PERIOD END DATE: December 31, 2016

REPORT FREQUENCY: Quarterly

Signed:

Hugh Daigle

ACCOMPLISHMENTS

The project **goal** is to show, through numerical modeling, how the transport of methane, and the mechanism by which it is transported, control the development of persistent, massive hydrate accumulations in deep sediments below the seabed. The models will be based on recently collected data from Walker Ridge Block 313 (WR 313) in the northern Gulf of Mexico (Figure 1). To achieve the project goal, the project has been divided into three phases. Phase 1 of the project will focus on modifying an existing reservoir simulator (Sun and Mohanty, 2006) to include microbial methane production, salt mass balance and effects on methane stability, and sedimentation. Additional 1-D modeling will provide constraints on expected rates of methanogenesis. Phase 2 of the project will focus on simulations of dissolved methane migration mechanisms to determine if sufficient flux is available to develop the massive hydrate accumulations observed at WR 313. Phase 3 of the project will focus on simulations of free methane gas migration and recycling of methane in the gas phase as it is buried below the base of the methane hydrate stability zone.

The **objectives** of this project are to define:

1. The dissolved methane flux, organic matter abundance, and time required to develop the accumulations observed at WR 313 by short-distance migration of microbial methane into adjacent coarser-grained layers;
2. The dissolved methane flux and time required to develop the accumulations observed at WR 313 by long-distance, updip migration;
3. Whether there is enough methane in the dissolved phase in the fine-grained sediments to form the observed hydrate deposits or whether a gas phase is present, and if so what the conditions are for three-phase equilibrium;
4. The fate of hydrate that subsides beneath the base of the MHSZ and accumulates as gas, and overpressure generation associated with gas accumulation.

Tasks to be performed
PHASE 1 / BUDGET PERIOD 1
Task 1 - Project management and planning

The Recipient shall work together with the DOE project officer upon award to develop a project management plan (PMP). The PMP shall be submitted within 30 days of the award. The DOE Project Officer shall have 20 calendar days from receipt of the PMP to review and provide comments to the Recipient. Within 15 calendar days after receipt of the DOE's comments, the Recipient shall submit a final PMP to the DOE Project Officer for review and approval.

The Recipient shall review, update, and amend the PMP (as requested by the DOE Project Officer) at key points in the project, notably at each go/no-go decision point and upon schedule

variances of more than 3 months and cost variances of more than 10%, which require amendments to the agreement and constitutes a re-base lining of the project.

The PMP shall define the approach to management of the project and include information relative to project risk, timelines, milestones, funding and cost plans, and decision-point success criteria. The Recipient shall execute the project in accordance with the approved PMP covering the entire project period. The Recipient shall manage and control project activities in accordance with their established processes and procedures to ensure subtasks and tasks are completed within schedule and budget constraints defined by the PMP. This includes tracking and reporting progress and project risks to DOE and other stakeholders.

Task 2 – Reservoir Model Development

The Recipient shall modify an existing general purpose reservoir simulator to include sedimentation, microbial methane production and effect of salt on hydrate equilibrium. The methane equilibrium calculation shall be modified to include changes in water activity due to dissolved salt following the method of Handa (1990). The mass conservation calculation shall be modified to include sedimentation, burial, and changes in porosity over time following the method of Bhatnagar et al. (2007). The initial conditions shall be modified to allow specification of heterogeneous properties (e.g., porosity) throughout the model domain. The boundary conditions shall be modified to allow specification of seafloor sedimentation rate and fluid flux. The Recipient shall verify code modifications with benchmark comparisons of performance with published simulation results (e.g., Bhatnagar et al., 2007).

Task 3 – 1-D Modeling of Microbial Methanogenesis

Concurrently with Task 2, the Recipient shall start with a 1-D reaction-transport model that will follow the burial by sedimentation of a sand layer surrounded by fine-grained sediments. The time-dependent modeling shall track the evolution of gas hydrate formation in the sand layer and shall provide more accurate estimates of the time scales and of the gas hydrate quantities associated with short migration. The methane hydrate stability conditions shall include the effect of pore size in the sand and fine-grained layers following the method of Malinverno (2010). The rate and spatial distribution of microbial methanogenesis shall be constrained by data from scientific ocean drilling expeditions (DSDP, ODP, IODP). The results of this task shall provide first-order constraints on rates of methanogenesis which shall be used as inputs to subsequent tasks (4.1, 4.3, 5.1, 5.2).

PHASE 2 / BUDGET PERIOD 2
Task 4.1 – Short Migration of Dissolved Methane

The Recipient shall investigate short migration of dissolved methane, in which methane generated in fine-grained sediments within the MHSZ is transported by diffusion into adjacent coarse-grained layers in which it forms concentrated hydrate deposits. The simulator developed in Task 2 shall be used for this task. The model domain shall consist of dipping sand layers surrounded by fine-grained sediments. This domain shall be designed to approximate the geometries observed at WR313 with sediment physical properties defined from logs or analog data. Rates of microbial methanogenesis and fluid flow shall be altered to determine the effect each has on the resulting hydrate distribution and time required for accumulation. The model results shall be used to determine the time scale of short migration at WR313, and the distribution of hydrate resulting from short migration.

Task 4.2 – Long Migration of Dissolved Methane

The Recipient shall investigate long migration of dissolved methane, in which dissolved methane is transported by advection from a distant source to the MHSZ. The investigation shall use the simulator developed in Task 2. The model domain shall consist of dipping sand layers surrounded by fine-grained sediments, and shall be designed to approximate the geometries observed at WR313. The model shall assume no local methane generation in the MHSZ and pore water entering the MHSZ with a methane concentration equal to the local solubility. Fluid flux shall be determined assuming that fluid flow is driven by overpressures to due high sedimentation rates (Gordon and Flemings, 1998). The Recipient shall explore the time scale associated with long migration by determining how long is required for fluid flow to form hydrate deposits comparable to those observed at WR313. The Recipient shall additionally simulate situations in which active fluid flow ceases after some time, and investigate how the hydrate that is formed evolves after cessation of fluid flow.

Task 4.3 – Assessment of Flux Associated with Dissolved Methane Migration

The Recipient shall use the model results from Tasks 4.1 and 4.2 to assess the methane flux associated with methane migration in the dissolved phase by either long or short migration. The different scenarios modeled in Tasks 4.1 and 4.2 shall be analyzed to determine methane flux from each migration mechanism, and the time scales and hydrate volumes produced by each. The analysis results shall be compared to the observed hydrate accumulations at WR313 and the age of the host sediments to determine whether migration of dissolved methane could have produced the observed hydrate accumulations.

PHASE 3 / BUDGET PERIOD 3
Task 5.1 – Assessment of Methane Budget Required for Presence of Gas Phase

The Recipient shall use the results of Tasks 4.1 and 4.2 to define methane availability from local, microbial sources as well as deeper sources (thermogenic or microbial). The phase equilibrium implemented in the 3-D model in Task 2 shall be used to determine local solubility within the model domain and determine the amount of methane that may be present as a gas phase. The results of this task will be used to place limits on gas availability in Tasks 5.2 and 5.3.

Task 5.2 – Free Gas Migration

The Recipient shall apply a previously established model of hydrate formation (multiphase-flow-controlled, nonequilibrium, neglecting transport of salinity and latent heat) to assess whether the gas phase accumulated beneath the MHSZ can contribute significantly to hydrate saturations within the MHSZ. The Recipient shall evaluate the conditions under which the accumulated gas phase drains into coarse-grained sediment. Having identified those conditions, the Recipient shall evaluate the geologic setting (dip angle, petrophysical properties and multiphase flow properties of the sediment) for which significant updip migration of the gas phase can be expected. The Recipient shall apply the hydrate formation model to geologic settings with significant expected migration to determine the hydrate saturation distribution in the updip direction. The model shall be tested for ranges of the two competing rates (namely, rate of gas accumulation at base of MHSZ and rate of hydrate formation from gas phase and water phase in the MHSZ). The Recipient shall additionally determine the pressure, temperature, and salinity conditions that will permit short migration of a gas phase within the MHSZ. The predicted saturation distributions shall be compared to observations (magnitude of hydrate saturation and its lateral extent) within coarse-grained layers at WR313. If hydrate is predicted to form in the same location and same volume as the accumulations observed at WR313, the Recipient shall determine whether the conditions that give agreement are geologically plausible, and the Recipient shall compare the flux of methane in the gas phase to the fluxes of methane by other mechanisms to be determined in Tasks 4.1 and 4.2. If the rates of methane delivery and time scale of hydrate accumulation are consistent with the accumulations observed at WR313, the Recipient shall use the results to guide the inclusion of free-gas migration phenomena into the full-physics 3D simulations of Task 5.3.

Task 5.3 – Methane Recycling at the Base of the MHSZ

The Recipient shall use the reservoir model developed in Task 2 to evaluate the fate of hydrate that moves below the base of the MHSZ as a result of sedimentation. In particular, the Recipient shall examine subsidence of dipping, hydrate-bearing sands of the type encountered at WR313. The Recipient shall model burial of a dipping sand layer through the base of the MHSZ in 3 dimensions. The Recipient shall test different scenarios of sedimentation rate, hydrate saturation in sand layers, and deep methane flux to evaluate gas accumulation below the MHSZ, supply of methane to the base of the MHSZ, and overpressure generated by the accumulation of a

connected gas column. The gas column will be considered connected when it overcomes a percolation threshold of roughly 10% of the pore volume (England et al., 1987). Gas phase pressure shall be computed from gas column height and estimates of capillary pressure from analog sediments (e.g., Blake Ridge; Clennell et al., 1999). The potential to fracture overlying sediments shall be investigated by comparing the resulting pore pressure to the total vertical stress and the minimum horizontal stress.

Milestone Status Report

1.A Title: PMP submission
Planned Date: 4 December 2013
Completed Date: 22 November 2013
Verification Method: Submission of final Project Management Plan to DOE within 65 days of start of project.

1.B Title: Project kick-off meeting
Planned Date: 29 December 2013
Completed Date: 7 November 2013
Verification Method: Meeting held within 90 days of start of project.

1.C Title: Sedimentation, microbial methane production, salinity effect implementation
Planned Date: 30 June 2014
Completed Date: 30 June 2014
Verification Method: Implementation of sedimentation, microbial methane production, salinity effect on hydrate stability in 3-D model.

1.D Title: Benchmarking of numerical model against published results
Planned Date: 31 March 2015
Completed Date: 31 March 2015
Verification Method: Simulation results match those obtained from other simulators in 1-D and 2-D (e.g., Bhatnagar et al., 2007; Chatterjee et al., 2011) within 1% in time and hydrate saturation using the same input parameters.

1.E Title: Development of time and methanogenesis constraints for future modeling
Planned Date: 31 March 2015
Completed Date: 31 March 2015
Verification Method: Development of a model that includes time-dependent changes in methane stability in a dipping, subsiding sand layer but matches the results of Cook and Malinverno (2013) for steady-state conditions.

2.A Title: Completion of short migration modeling
Planned Date: 30 September 2016
Completed Date: 30 September 2016
Verification Method: Completion of simulations to evaluate conditions necessary for development of massive hydrate deposits by short migration.

2.B Title: Completion of long migration modeling
Planned Date: 30 September 2016
Completed Date: 30 September 2016
Verification Method: Completion of simulations to evaluate conditions necessary for development of massive hydrate accumulations by long migration.

2.C Title: Quantification of methane flux in the dissolved phase
Planned Date: 30 September 2016
Completed Date: 30 September 2016
Verification Method: Quantification of methane flux associated with methane migration in the dissolved phase by either long or short migration and comparison with existing estimates of methane flux in the northern Gulf of Mexico such as those presented in Frye (2008).

3.A Title: Quantification of methane availability and expected quantities of gas
Planned Date: 30 September 2017
Verification Method: Quantification of amount of methane required to form a free gas phase and comparison with existing estimates of methane flux in the northern Gulf of Mexico such as those presented in Frye (2008).

3.B Title: Completion of free gas migration models
Planned Date: 30 September 2017
Verification Method: Determinations of methane flux and time necessary to reproduce observed hydrate accumulations at WR313 by migration of free gas.

3.C Title: Completion of modeling efforts to assess methane recycling
Planned Date: 30 September 2017
Verification Method: Completion of simulations to assess rates of gas accumulation beneath MSHZ and effect on gas migration and overpressure generation.

What was accomplished under these goals?

Major activities

Work commenced on Tasks 5.1, 5.2, and 5.3. We developed a rock physics model to enable us to investigate the relationship between the character of the bottom simulating reflection (BSR) and the amount of methane present as gas, hydrate, or a dissolved phase at the base of hydrate stability.

There are two models that may be used to describe the acoustic behavior of hydrate-bearing sediments. The first model, the contact-cement model, assumes that hydrate has cemented the grain contacts as shown in Figure 1a below. In this model, hydrate acts similarly to cement, giving additional mechanical strength to the sediments. Using this model will greatly increase the elastic moduli of the rock frame with the addition of hydrate. The second model, the no-contact-cement model (Figure 1b), assumes that the hydrate is deposited away from grain contacts. In this model, hydrate is generated within the pore fluid and the elastic moduli of the sediment frame are not affected by its presence. These physical rock models link the elastic wave velocities in high-porosity sediments to porosity, density, effective pressure, mineralogy and fluid saturation.

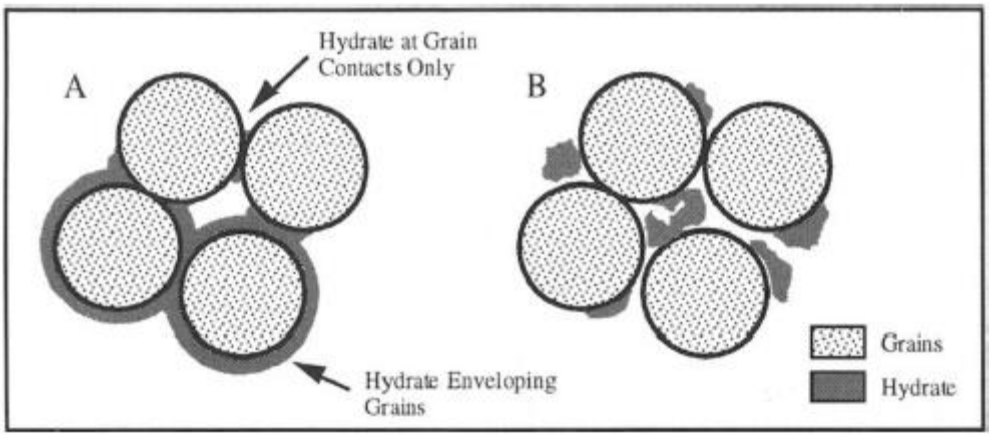

Figure 1. Model A, the contact-cement model, assumes that hydrate cements the grain evenly. Model B, the no-contact-cement model for hydrate deposition among the grains (Ecker et al., 1998).

Ecker et al. (1998) concluded that hydrate does not cement the grain contacts as only the no-contact-cement model could qualitatively reproduce the observed amplitude versus offset (AVO) response. Since no contact-cement model best represents the hydrate deposition among grains, this model makes rock physics analysis for next steps much simpler.

The bulk and shear moduli, K and G respectively, can be used to directly relate changes in lithology and hydrate saturation to mechanical properties. These two parameters are related to the acoustic velocities by:

$$G = \rho V_s^2, \text{ (Eq. 1)}$$

$$K = \rho\left(V_p^2 - \frac{4}{3}V_s^2\right), \text{ (Eq. 2)}$$

where ρ is the density of the formation, V_p is compressional velocity, and V_s is shear velocity. The acoustic velocities can be determined by rearranging Equations (1) and (2) as

$$V_p = \sqrt{\frac{K_{sat}+\frac{4}{3}G_{sat}}{\rho_B}}, \text{ (Eq. 3)}$$

$$V_s = \sqrt{\frac{G_{sat}}{\rho_B}}, \text{ (Eq. 4)}$$

$$\rho_B = (1-\emptyset)\rho_s + \emptyset\rho_f, \text{ (Eq. 5)}$$

where ∅ is porosity, ρ_s is the bulk density of the solid phase and ρ_f is the density of the pore fluid.

Gassmann's (1951) equations express the bulk and shear modulus as functions of the elastic moduli of rock minerals and fluids and their relative abundances. These equations may be used to calculate the acoustic velocity changes as a result of substitution of the fluid saturations in pore space. Therefore, these equations provide a framework for describing the changes in elastic properties as hydrate or gas saturation change. Gassmann's equations express the saturated bulk and shear moduli K_{sat} and G_{sat} as

$$K_{sat} = K\frac{\emptyset K_{dry} - \frac{(1+\emptyset)K_f K_{dry}}{K} + K_f}{(1-\emptyset)K_f + \emptyset K - \frac{K_f K_{dry}}{K}}, \text{ (Eq. 6)}$$

$$G_{sat} = G_{dry}, \text{ (Eq. 7)}$$

where K is the bulk modulus of the matrix/rock (solid mineral grains), K_f is the bulk modulus of the pore fluid (Section 2.3.1), K_{dry} and G_{dry} are the dry bulk and shear moduli of the rock, and ∅

is the porosity. The shear modulus is independent of fluid saturation (Berryman, 1999). The modified Hashin-Shtrikman-Hertz-Mindlin theory (Dvorkin et al., 1999) can be used to find the bulk and shear moduli of the dry frame (K_{dry} and G_{dry}). This theory first calculates the effective bulk and shear moduli at a critical porosity using the Hertz Mindlin theory (Mindlin, 1949). Critical porosity ($\emptyset_c$) can vary between 36% and 40%; these two values represent the porosity of a random dense pack of spherical grains. The critical porosity separates the mechanical and acoustic behavior into two distinct regions (Nur et al., 1998): for porosities lower than $\emptyset_c$, the mineral grains are load bearing, while for porosities greater than $\emptyset_c$, the sediment becomes a suspension, with the fluid phase becoming load-bearing. The effective moduli at the critical porosity are given by:

$$K_{HM} = \left[\frac{G^2 n^2 (1-\emptyset_c)^2}{18\pi^2(1-\nu)^2} P\right]^{\frac{1}{3}}, \text{(Eq. 8)}$$

$$G_{HM} = \frac{5-4\nu}{5(2-\nu)}\left[\frac{3G^2 n^2 (1-\emptyset_c)^2}{2\pi^2(1-\nu)^2} P\right]^{\frac{1}{3}}, \text{(Eq. 9)}$$

where n is the average number of contacts per grain that varies between 4 and 10 depending on compaction and consolidation. For relatively compacted and consolidated formations value this value is taken to be 8.5 (Murphy, 1982). A value of 9 can be used for close packing. ν is the Poisson's ratio of the mineral phase calculated from K and G as following:

$$\nu = \frac{3K-2G}{2(3K+G)}, \text{(Eq. 10)}$$

If the sediment rock consists of a mixed mineralogy, the bulk and shear moduli K and G of the rock can be determined using a Hill's average formula:

$$K = \frac{1}{2} * [\sum_{i=1}^{m} f_i K_i + (\sum_{i=1}^{m} \frac{f_i}{K_i}^{-1})], \text{(Eq. 11)}$$

$$G = \frac{1}{2} * [\sum_{i=1}^{m} f_i K G_i + (\sum_{i=1}^{m} \frac{f_i}{G_i}^{-1})], \text{(Eq. 12)}$$

where m is number of different mineral components, f_i is the volumetric fraction of the i^{th} component in the rock, and K_i and G_i are the bulk and shear moduli of the i^{th} component,

respectively. An alternate approach to Hill's average may be employed by expressing the elastic moduli of the grains as a linear combination of two endmembers whose volume fractions are defined by the gamma ray log (e.g., Guerin et al., 1999).

Guerin et al. (1999) uses the Voigt-Reuss-Hill average of the grain moduli of the two main mineral phases of sand (K_s and G_s) and clay (K_c and G_c).The grain bulk modulus can be calculated by:

$$K = \frac{1}{2}\left[\gamma K_c + (1-\gamma)K_s + \frac{K_s K_c}{K_s\gamma + K_c(1-\gamma)}\right], \text{(Eq. 13)}$$

$$G = \frac{1}{2}\left[\gamma G_c + (1-\gamma)G_s + \frac{G_s G_c}{G_s\gamma + G_c(1-\gamma)}\right], \text{(Eq. 14)}$$

where γ is normalized gamma ray values and it is used to define the clay mineral percentage in the sediments.

K_f is identical to the bulk modulus of water, in the case of purely brine-saturated sediments. If the sediment is homogeneously saturated with gas, K_f becomes an isostress average of water (K_w) and gas (K_g) at saturation S_w. As mentioned before, the no-contact-cement model assumes that the hydrate is deposited away from grain contacts. Hydrate is generated within the pore fluid and the elastic properties of the sediment are not affected or subjected to change. Similarly to the sediment without gas hydrate, the pore fluid will consist of a mixture of brine, hydrate, and gas. Therefore, for the case of hydrate being part of pore fluid, the bulk modulus of the fluid is the isostress average of water, hydrate, and gas. The bulk modulus of the fluid is calculated from following equation:

$$K_f = \left[\frac{S_w}{K_w} + \frac{S_h}{K_h} + \frac{S_g}{K_s}\right]^{-1}. \text{(Eq. 15)}$$

Modified Hashin-Shtrikman upper and lower bound is then used to calculate the dry moduli of the solid phase for porosities above and below the critical porosity (Dvorkin and Nur, 1996; Ecker et al., 1998). If the porosity is below the critical porosity of 40%, the dry moduli can be calculated as

$$K_{dry} = \left[\frac{\frac{\emptyset}{\emptyset_c}}{K_{HM}+\frac{4}{3}G_{HM}} + \frac{1-\frac{\emptyset}{\emptyset_c}}{K+\frac{4}{3}G_{HM}}\right]^{-1} - \frac{4}{3}G_{HM}, \text{(Eq. 16)}$$

$$G_{dry} = \left[\frac{\frac{\emptyset}{\emptyset_c}}{G_{HM}+Z} + \frac{1-\frac{\emptyset}{\emptyset_c}}{G+Z}\right]^{-1} - Z, \text{(Eq. 17)}$$

$$Z = \frac{G_{HM}}{6}\left[\frac{9K_{HM}+8G_{HM}}{K_{HM}+2G_{HM}}\right]. \text{(Eq. 18)}$$

If the porosity is above the critical porosity of 40%, the dry moduli can be calculated as

$$K_{dry} = \left[\frac{\frac{1-\emptyset}{1-\emptyset_c}}{K_{HM}+\frac{4}{3}G_{HM}} + \frac{\frac{1-\emptyset}{1-\emptyset_c}}{\frac{4}{3}G_{HM}}\right]^{-1} - \frac{4}{3}G_{HM}\text{ , (Eq. 19)}$$

$$G_{dry} = \left[\frac{\frac{1-\emptyset}{1-\emptyset_c}}{G_{HM}+Z} + \frac{\frac{1-\emptyset}{1-\emptyset_c}}{Z}\right]^{-1} - Z. \text{(Eq. 20)}$$

The model derived by Wood (1941) considers the mechanical behavior of unconsolidated sediments as particles in suspension. The dry bulk modulus by Wood is determined as

$$K_{dry-Wood} = \frac{KK_f}{\emptyset K+K_f(1-\emptyset)}, \text{ (Eq. 21)}$$

where K is the weighted average of the compressibility of the grain aggregate, and K_f is the weighted average of the compressibility of the pore fluid.

Hamilton (1971) established a relationship between the dry bulk modulus and the porosity of marine sediments. He defined two different relationships for fine sand and silt-clay as following:

$$\log\left(K_{dry}(*10^{-9}Pa)\right) = 1.7093 - 4.25391\emptyset, \text{(Eq. 22)}$$

$$\log\left(K_{dry}(*10^{-9}Pa)\right) = 1.7358 - 4.25075\emptyset, \text{(Eq. 23)}$$

with ∅ expressed in decimal fraction. It has to be mentioned that the first terms on the right of these two equations represent the logarithm of the grain bulk modulus *K*, which is equal to the dry bulk modulus at zero porosity. Furthermore, these two distinct relationships can be defined to a single formula for elastic sediments:

$$\log(K_{dry}) = \log(K) - 4.25\emptyset \text{ (Eq. 24)} \quad \text{or} \quad \log\left(\frac{K_{dry}}{K}\right) = -4.25\emptyset. \text{ (Eq. 25)}$$

Solving for K_{dry} for more ease of use, we would have:

$$K_{dry} = K * 10^{-4.25\emptyset}. \text{ (Eq. 26)}$$

This generalization ensures that the frame bulk modulus equals the grain bulk modulus at ∅=0 for any value of the aggregate grain modulus. Furthermore, combination of Hamilton's and Gassmann's equation is referred as the Gassmann-Hamilton Model.

Minerology takes an important role in the properties of sediment, and therefore it is required to have knowledge the minerology of the sediments. Different sites around the world have different minerology, which may change the approaches for to a solution. For example, Ecker et al. (2000) used a homogeneous model where formation consisted of 60% clay, 35% calcite and 5% quartz for all layers. For this study, since the sediments at Walker Ridge are dominantly clay and quartz, a normalized gamma ray was used to calculated the bulk and shear moduli of the formation. This means that, every single depth in the well has its own unique set of shear and bulk moduli. Properties used for calculation are shown in Table 1.

Components	Density [g/cm^3]	Vp [m/s]	Vs [m/s]	K (GPa)	G (GPa)
Clay	2.6	3400	1600	21.2	6.667
Sand/CaCO3	2.7	5980	4040	38	44
Gas hydrate	0.9	3300	1680	6.414	2.54
Water	1.05	1600	0	2.688	0
Gas	0.3	849	0	0.216	0

Table 1. Component properties used for calculations.

We modeled the change in elastic properties with phase saturation in a three-phase zone at Walker Ridge. This includes variation of hydrate and gas saturation between 1% to 5% and zero to 50% respectively for a three-phase zone with 5 meter thickness. The hydrate stability zone is located at 882 meters below the seafloor (mbsf) in sandy layers and at 885 mbsf in clay layers (Bihani, 2016). For ease of work depth of 880 mbsf was used as the base for fluid substitution.

Note: In all figures presented, the annotation (e.g. 69-01-30-5) indicated the saturation and thickness of the 3-phase zone. These annotations refer to water saturation, hydrate saturation, gas saturation, and thickness respectively. For example, annotations 69-01-30-5, indicates water saturation of 69%, hydrate saturation of 1%, free gas saturation of 30%, and 3-phase zone thickness of 5 meters.

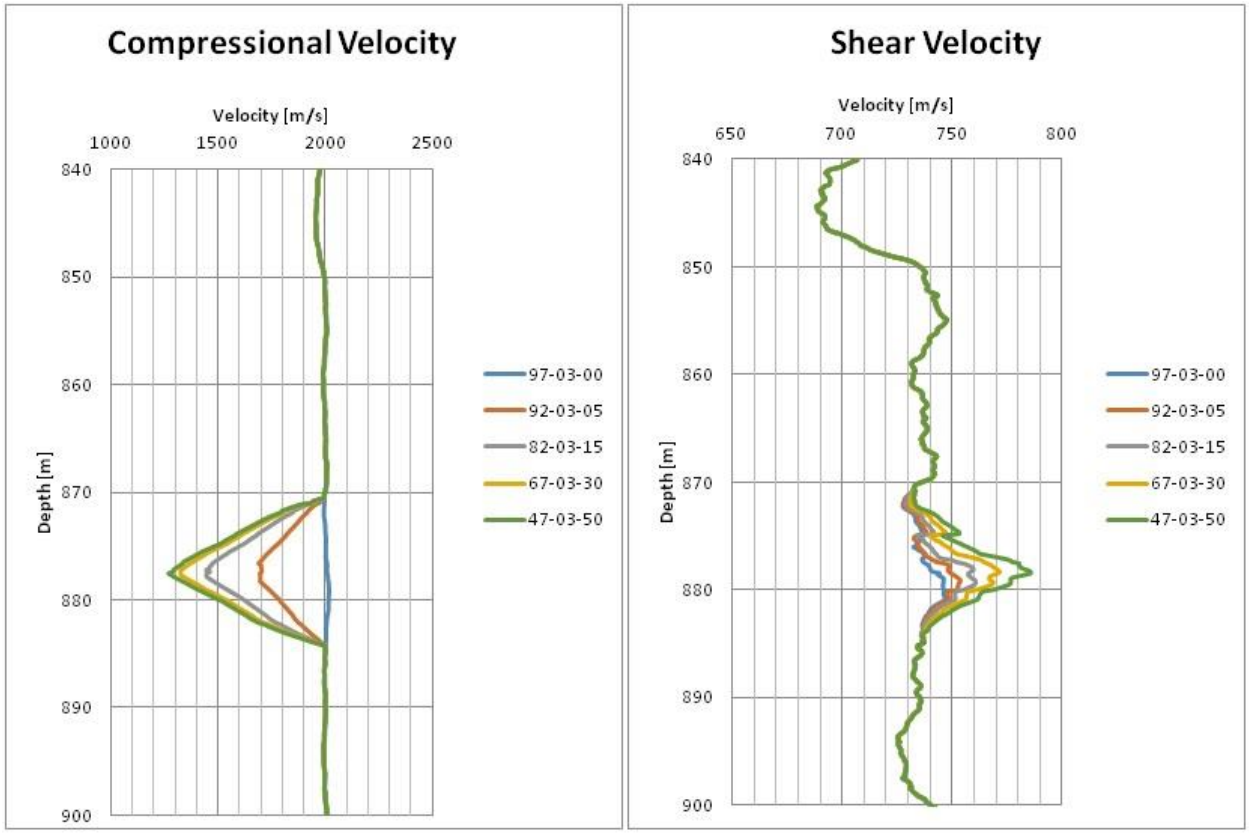

Figure 3. Compressional (left) and shear (right) velocities for a case where the hydrate saturation is 3% in a 5 m-thick three-phase zone with increasing gas saturation.

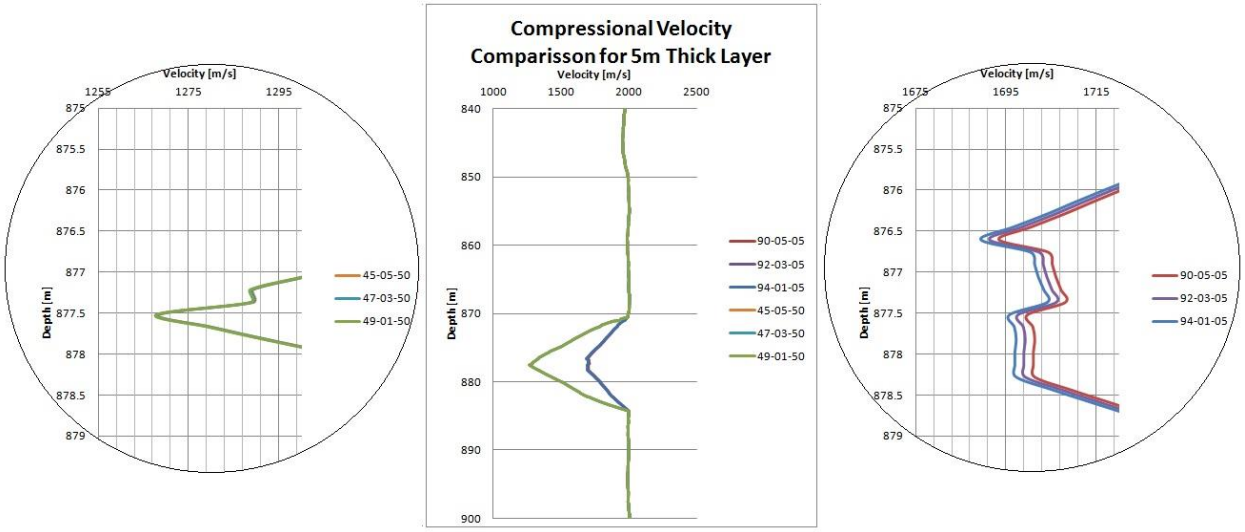

Figure 4. At high gas saturation (left), the hydrate saturation does not affect the compressional velocity. However, at low gas saturation (5%, right), small changes in hydrate saturation do influence compressional velocity.

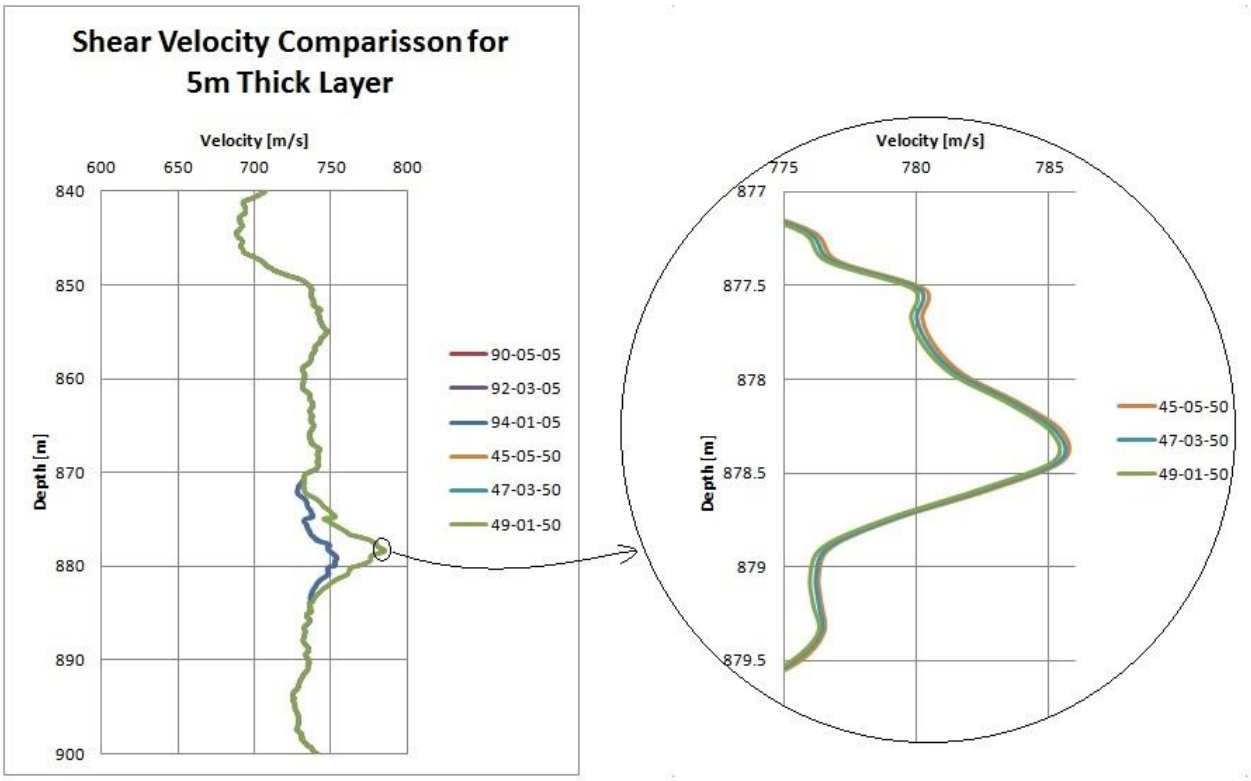

Figure 5. Shear velocities for the case presented in Figure 4.

Based on the information shown in Figs. 3-5, it can be seen that the gas content of the three-phase zone is the main driver of changes in elastic properties. The hydrate saturation is only important when gas saturation is very low.

Li Wei worked to reformat her 1D model to Semi-Lagrangian, with help from the detailed text written by Alberto Malinverno. We are still working on this model, but are nearly done with the base. This model will be used in the ICGH presentation in summer 2017. Jess Hillman and Ann Cook continued to work on a paper about methane migration mechanisms in thin sands and fine-grained units in the Terrebonne basin; co-authors include Hugh Dangle, Michael Nole and Alberto Malinverno. Ann, Alberto, and Hugh along with lead chair Kehua You represented the project together by hosting an AGU session on natural gas hydrates.

Malinverno applied a time-dependent reaction-transport model to compute predicted gas hydrate contents in fine-grained sediments. Microbial methanogenesis in these sediments can contribute to the accumulation of hydrates in adjacent coarse-grained layers. The goal of this modeling work is to test whether a transient period of high organic carbon deposition at the seafloor can result in a sediment interval with more intense methane generation and enhanced hydrate formation. The modeling was successful in predicting gas hydrate amounts close to those estimated at 170-310 mbsf in the JIP Walker Ridge 313-H site, where hydrates formed in near-

vertical fractures. These results were presented at 2016 Fall meeting of the American Geophysical Union in San Francisco.

Specific objectives

None for this quarter

Significant results and key outcomes

What opportunities for training and professional development has the project provided?

PI Daigle and co-PI Mohanty have been working with PhD student Michael Nole and MS student Ryan Leung on various aspects of pore-scale modeling of methane hydrate systems. This work has involved weekly meetings and independent work.

Co-PIs Cook and Malinverno have been working with PhD student Li Wei on modeling microbial methanogenesis. This work has involved weekly meetings and independent work.

How have the results been disseminated to communities of interest?

Two presentations were made at the American Geophysical Union Fall Meeting.

Plans during next reporting period to accomplish goals

Work will continue on Tasks 5.1, 5.2, and 5.3.

PRODUCTS

Malinverno, A., Cook, A., Daigle, H., 2016. Modeling the formation of hydrate-filled veins in fine-grained sediments from in situ microbial methane. Presented at the American Geophysical Union Fall Meeting, San Francisco, CA, 12-16 December 2016. Federal support acknowledged.

Nole, M., Daigle, H., Cook, A., Malinverno, A., Hillman, J.I.T., 2016. Linking pore-scale and basin-scale effects on diffusive methane transport in hydrate bearing environments through multi-scale reservoir simulations. Presented at the American Geophysical Union Fall Meeting, San Francisco, CA, 12-16 December 2016. Federal support acknowledged.

Shushtarian, A., 2016. Effect of a discrete three-phase methane equilibrium zone on the bottom-simulating reflection. M.S. thesis, Department of Petroleum and Geosystems Engineering, University of Texas, Austin, TX. Federal support acknowledged.

PARTICIPANTS AND OTHER COLLABORATING ORGANIZATIONS

Name: Hugh Daigle
Project role: PI
Nearest person month worked: 1
Contribution to project: Project management; assisted with code development
Collaborated with individual in foreign country: No

Name: Kishore Mohanty
Project role: Co-PI
Nearest person month worked: 1
Contribution to project: Assisted with code development
Collaborated with individual in foreign country: No

Name: Steven Bryant
Project role: Co-PI
Nearest person month worked: 1
Contribution to project: Assisted with code development
Collaborated with individual in foreign country: No

Name: Michael Nole
Project role: Graduate Student
Nearest person month worked: 3
Contribution to project: Primary worker on developing computer code
Collaborated with individual in foreign country: No

Name: Ann Cook
Project role: Co-PI
Nearest person month worked: 1
Contribution to project: Worked on gathering specific data for modeling of microbial methanogenesis, developing methanogenesis code
Collaborated with individual in foreign country: No

Name: Li Wei
Project role: Graduate Student
Nearest person month worked: 3
Contribution to project: Worked on developing methanogenesis code
Collaborated with individual in foreign country: No

Name: Alberto Malinverno
Project role: Co-PI
Nearest person month worked: 1
Contribution to project: Provided data for microbial methanogenesis modeling
Collaborated with individual in foreign country: No

IMPACT

What is the impact on the development of the principal discipline of the project?

The central focus of this project is refining our understanding of the methane migration pathways that feed methane hydrate deposits in marine sediments. Understanding migration pathways is an important component of understanding methane hydrates as a petroleum system, a necessary step towards prospecting for economically recoverable hydrate deposits. Additionally, our results will help refine our understanding of the carbon cycle in marine sediments, and specifically how methane is transported and sequestered.

What is the impact on other disciplines?

The results of this project will be important for other engineering disciplines in which researchers are developing methods for extracting methane from the subsurface since it will provide information on how methane is distributed in sediments at different scales. In addition, the results will be of interest to the economics and risk assessment fields since we will develop methods to determine more precisely how much hydrate may be present in subsurface reservoirs.

What is the impact on the development of human resources?

This project will provide funding for three graduate students to conduct collaborative research on methane hydrates and give them an opportunity to participate in important hands-on learning experiences outside the classroom.

What is the impact on physical, institutional, and information resources that form infrastructure?

Our results may be used for better design of subsea oil and gas infrastructure since more precise assessment of hydrate resources will allow better assessment of hydrates as a hazard. In addition, production infrastructure specifically for hydrate reservoirs may be improved by our results since we will allow more accurate determination of the volumes of methane expected to exist in the subsurface.

What is the impact on technology transfer?

Our results will be disseminated at conferences and in peer-reviewed publications.

What is the impact on society beyond science and technology?

The impact of this work on society will be twofold. First, the better understanding of hydrates in a petroleum systems framework will allow for more efficient production of natural gas from these deposits, which will provide an additional energy resource. Second, the better understanding of methane cycling and distribution in the subsurface will influence regulatory decisions involving hydrates as geohazards or climate change agents.

What dollar amount of the award's budget is being spent in foreign country(ies)?
None

CHANGES/PROBLEMS
None

SPECIAL REPORTING REQUIREMENTS
None

BUDGETARY INFORMATION
See attached spreadsheet.

References

Berryman, J.G., 1999. Origin of Gassmann's equations. Geophysics, 64(5), 1627-1629.
Bhatnagar, G., Chapman, W.G., Dickens, G.R., Dugan, B., Hirasaki, G.J., 2007. Generalization of gas hydrate distribution and saturation in marine sediments by scaling of thermodynamic and transport processes. Am. J. Sci., 307, 861-900.
Bihani, A., 2016. Pore size distribution and methane equilibrium conditions at Walker Ridge Block 313, northern Gulf of Mexico. MS thesis, Department of Petroleum and Geosystems Engineering, University of Texas, Austin, TX.
Chatterjee, S., Dickens, G.R., Bhatnagar, G., Chapman, W.G., Dugan, B., Snyder, G.T., Hirasaki, G.J., 2011. Pore water sulfate, alkalinity, and carbon isotope profiles in shallow sediment above marine gas hydrate systems: A numerical modeling perspective. J. Geophys. Res., 116(B9), B09103.
Clennell, M.B., Hovland, M., Booth, J.S., Henry, P., Winters, W.J., 1999. Formation of natural gas hydrates in marine sediments 1. Conceptual model of gas hydrate growth conditioned by host sediment properties. J. Geophys. Res., 104(B10), 22985-23003.

Cook, A.E., Malinverno, A., 2013. Short migration of methane into a gas hydrate-bearing sand layer at Walker Ridge, Gulf of Mexico. Geochem. Geophys. Geosyst., 14(2), 283-291.
Dvorkin, J., Nur, A., 1996. Elasticity of high-porosity sandstones: Theory for two North Sea data sets. Geophysics, 61(5), 1363-1370.
Dvorkin, J., Prasad, M., Sakai, A., Lavoie, D., 1999. Elasticity of marine sediments: Rock physics modeling. Geophys. Res. Lett., 26(12), 1781-1784.
Ecker, C., Dvorkin, J., Nur, A., 1998. Sediments with gas hydrates: Internal structure from seismic AVO. Geophysics, 63(5), 1659-1669.
Ecker, C., Dvorkin, J., Nur, A., 2000. Estimating the amount of gas hydrate and free gas from marine seismic data. Geophysics, 65(2), 565-573.
England, W.A., Mackenzie, A.S., Mann, D.M., Quigley, T.M., 1987. The movement and entrapment of petroleum fluids in the subsurface. J. Geol. Soc. London, 144, 327-347.
Frye, M., 2008. Preliminary evaluation of in-place gas hydrate resources: Gulf of Mexico Outer Continental Shelf. Minerals Management Service Report 2008-004. Available online at: http://www.boem.gov/uploadedFiles/BOEM/Oil_and_Gas_Energy_Program/Resource_Evaluation/Gas_Hydrates/MMS2008-004.pdf
Gassmann, F., 1951. Elastic waves through a packing of spheres. Geophysics, 16(4), 673-685.
Gordon, D.S., Flemings, P.B., 1998. Generation of overpressure and compaction-driven fluid flow in a Plio-Pleistocene growth-faulted basin, Eugene Island 330, offshore Louisiana. Basin Res., 10(2), 177-196.
Guerin, G., Goldberg, D., Meltser, A., 1999. Characterization of in situ elastic properties of gas hydrate-bearing sediments on the Blake Ridge. J. Geophys. Res., 104(B8), 17781-17795.
Hamilton, E.L., 1971. Elastic properties of marine sediments. J. Geophys. Res., 76(2), 579-604.
Handa, Y.P., 1990. Effect of hydrostatic pressure and salinity on the stability of gas hydrates. J. Phys. Chem., 94(6), 2652-2657.
Malinverno, A., 2010. Marine gas hydrates in thin sand layers that soak up microbial methane. Earth Planet. Sci. Lett., 292(3-4), 399-408.
Mindlin, R.D., 1949. Compliance of elastic bodies in contact. J. Appl. Mech., 16(3), 259-268.
Murphy, W.F.I., 1982. Effects of microstructure and pore fluids on the acoustic properties of granular sedimentary materials. PhD thesis, Department of Geophysics, Stanford University, Stanford, CA.
Nur, A., Mavko, G., Dvorkin, J., Galmudi, D., 1998. Critical porosity: A key to relating physical properties to porosity in rocks. Lead. Edge, 17(3), 357-362.

Baseline Reporting Quarter	Budget Period 1																	
	Q1		Q2		Q3		Q4		Q1		Q2		Q3		Q4			
	10/1/13 - 12/31/13		1/1/14 - 3/31/14		4/1/14 - 6/30/14		7/1/14 - 9/30/14		10/1/14 - 12/31/14		1/1/15 - 3/31/15		4/1/15 - 6/30/15		7/1/15 -			
	Q1	Cumulative Total	Q2	Cumulative Total	Q3	Cumulative Total	Q4	Cumulative Total	Q1	Cumulative Total	Q2	Cumulative Total	Q3	Cumulative Total	Q4			
Baseline Cost Plan																		
Federal Share	$ 97,167	$ 97,167	$ 97,167	$ 194,333	$ 97,167	$ 291,500	$ 97,167	$ 388,666	$ 97,167	$ 485,833	$ 97,167	$ 582,999	$ 108,258	$ 691,257	$ 108,258			
Non-Federal Share	$ 24,292	$ 24,292	$ 24,292	$ 48,583	$ 24,292	$ 72,875	$ 24,292	$ 97,167	$ 24,292	$ 121,458	$ 24,292	$ 145,750	$ 29,698	$ 175,447	$ 29,698			
Total Planned	$ 121,458	$ 121,458	$ 121,458	$ 242,916	$ 121,458	$ 364,374	$ 121,458	$ 485,833	$ 121,458	$ 607,291	$ 121,458	$ 728,749	$ 137,956	$ 866,704	$ 137,956			
Actual Incurred Cost																		
Federal Share	0	0	$ 4,053	$ 4,053	$ 59,844	$ 63,897	$ 135,066	$ 198,963	$ 113,678	$ 312,641	$ 174,686	$ 487,327	$ 36,292	$ 523,619	$ 179,321			
Non-Federal Share	0	0	0	0	$ -	$ -	$ 8,832	$ 8,832	$ 63,148	$ 71,980	$ 51,748	$ 123,728	$ 6,615	$ 130,343	$ 21,898			
Total Incurred Costs	0	0	0	0	$ 59,844	$ 63,897	$ 143,898	$ 207,795	$ 176,826	$ 384,621	$ 226,435	$ 611,056	$ 42,907	$ 653,963	$ 201,219			
Variance																		
Federal Share	$ (97,167)	$ (97,167)	$ (93,113)	$ (190,280)	$ (37,323)	$ (227,602)	$ 37,900	$ (189,703)	$ 16,512	$ (173,191)	$ 77,520	$ (95,672)	$ (71,966)	$ (167,638)	$ 71,063			
Non-Federal Share	$ (24,292)	$ (24,292)	$ (24,292)	$ (48,583)	$ (24,292)	$ (72,875)	$ (15,460)	$ (88,335)	$ 38,856	$ (49,478)	$ 27,457	$ (22,021)	$ (23,083)	$ (45,104)	$ (7,800)			
Total Variance	$ (121,458)	$ (121,458)	$ (117,405)	$ (238,863)	$ (61,614)	$ (300,477)	$ 22,440	$ (278,037)	$ 55,368	$ (222,670)	$ 104,977	$ (117,693)	$ (95,049)	$ (212,742)	$ 63,263			

Budget Period 2										Budget Period 3							
4	Q1		Q2		Q3		Q4		Q1		Q2		Q3		Q4	
9/30/15	10/1/15 - 12/31/15		1/1/16 - 3/31/16		4/1/16 - 6/30/16		7/1/16 - 9/30/16		10/1/16 - 12/31/16		1/1/17 - 3/31/17		4/1/17 - 6/30/17		7/1/17 - 9/30/17	
Cumulative Total	Q1	Cumulative Total	Q2	Cumulative Total	Q3	Cumulative Total	Q4	Cumulative Total	Q1	Cumulative Total	Q2	Cumulative Total	Q3	Cumulative Total	Q4	Cumulative Total
$ 799,515	$ 108,258	$ 907,773	$ 108,258	$ 1,016,031	$ 108,258	$ 1,124,289	$ 108,258	$ 1,232,547	$ 111,371	$ 1,343,918	$ 111,371	$ 1,455,290	$ 111,371	$ 1,566,661	$ 111,371	$ 1,678,032
$ 205,145	$ 29,698	$ 234,842	$ 29,698	$ 264,540	$ 29,698	$ 294,237	$ 29,698	$ 323,935	$ 30,888	$ 354,823	$ 30,888	$ 385,711	$ 30,888	$ 416,600	$ 30,888	$ 447,488
$ 1,004,660	$ 137,956	$ 1,142,615	$ 137,956	$ 1,280,571	$ 137,956	$ 1,418,526	$ 137,956	$ 1,556,482	$ 142,260	$ 1,698,741	$ 142,260	$ 1,841,001	$ 142,260	$ 1,983,260	$ 142,260	$ 2,125,520
$ 702,941	$ 142,071	$ 845,012	$ 112,450	$ 957,462	$ 85,549	$ 1,043,011	$ 133,581	$ 1,176,592	$ 88,083	$ 1,264,675						
$ 152,241	$ 21,898	$ 174,139	$ 14,224	$ 188,363	$ 72,390	$ 260,753	$ 38,937	$ 299,689	$ 83,650	$ 383,339						
$ 855,182	$ 163,969	$ 1,019,151	$ 126,674	$ 1,145,825	$ 157,939	$ 1,303,764	$ 172,518	$ 1,476,282	$ 171,732	$ 1,648,014						
$ (96,574)	$ 33,813	$ (62,761)	$ 4,192	$ (58,569)	$ (22,709)	$ (81,278)	$ 25,323	$ (55,955)	$ (23,289)	$ (79,243)						
$ (52,904)	$ (7,800)	$ (60,704)	$ (15,474)	$ (76,177)	$ 42,693	$ (33,485)	$ 9,239	$ (24,246)	$ 52,761	$ 28,516						
$ (149,478)	$ 26,014	$ (123,464)	$ (11,281)	$ (134,746)	$ 19,984	$ (114,762)	$ 34,562	$ (80,200)	$ 29,473	$ (50,728)						